Ann. Geophys., 33, 333–344, 2015
www.ann-geophys.net/33/333/2015/
doi:10.5194/angeo-33-333-2015

Annales Geophysicae
Open Access

Outflow of low-energy O^+ ion beams observed during periods without substorms

G. K. Parks[1], E. Lee[2], S. Y. Fu[3], M. Fillingim[1], I. Dandouras[4], Y. B. Cui[3], J. Hong[2], and H. Rème[4]

[1]Space Sciences Laboratory, University of California, Berkeley, CA, USA
[2]School of Space Research, Kyung Hee University, Yongin, Gyeonggi, Korea
[3]School of Earth and Space Sciences, Peking University, Beijing, China
[4]CNRS, IRAP, 9 Ave. Colonel Roche, Toulouse, France

Correspondence to: G. K. Parks (parks@ssl.berkeley.edu)

Received: 26 November 2014 – Revised: 6 February 2015 – Accepted: 25 February 2015 – Published: 17 March 2015

Abstract. Numerous observations have shown that ions flow out of the ionosphere during substorms with more fluxes leaving as the substorm intensity increases (Wilson et al., 2004). In this article we show observations of low-energy (few tens of electron volts) ionospheric ions flowing out periods without substorms, determined using the Wideband Imaging Camera (WIC) and Auroral Electrojet (AE) indices. We use Cluster ion composition data and show the outflowing ions are field-aligned H^+, He^+ and O^+ beams accelerated to energies of $\sim$ 40–80 eV, after correcting for spacecraft potential. The estimated fluxes of the low-energy O^+ ions measured at $\sim$ 20 000 km altitude are $> 10^3$–10^5 cm^{-2} s. Assuming the auroral oval is the source of the escaping ions, the measured fluxes correspond to a flow rate of $\sim 10^{19}$–10^{21} ions s^{-1} leaving the ionosphere. However, periods without substorms can persist for hours suggesting the low-energy ions flowing out during these times could be a major source of the heavy ion population in the plasma sheet and lobe.

Keywords. Magnetospheric physics (Magnetosphere–ionosphere interactions)

1 Introduction

The ionospheric ions that flow out into the magnetosphere include the polar wind, upwelling ions from the cusp, polar cap, and ion beams accelerated in the aurora by the electric field parallel to the magnetic field direction. These escaping ions have been observed by experiments from radars on the ground (Wahlund et al., 1992) and on numerous satellites including DE1, Polar, Geotail and Cluster (Yan and André, 1997; André and Yau, 1997; Moore et al., 1999; Maggiolo et al., 2006, 2011; Nilsson et al., 2006; Seki et al., 2001). The polar cap ions include the polar wind (Engwall et al., 2009; Li et al., 2012) and cusp origin O^+ (Nilsson et al., 2012; Liao et al., 2010, 2012). Cold polar cap ions sometimes consist of mainly H^+ ions and can dominate the lobe outflow fluxes (Engwall et al., 2009; Nilsson et al., 2010). Ions flowing out with transpolar arcs (TPAs, also known as theta auroras) are field-aligned and observed when the interplanetary magnetic field (IMF) is northward (Kullen, 2012). Case events and statistical studies have shown the ion beams flowing out of the polar cap are similar to auroral beams accelerated by field-aligned potentials (Maggiolo et al., 2006, 2011; Nilsson et al., 2004, 2006; Kronberg et al., 2014). However, cold O^+ beams may form from velocity dispersion, and the beams can look similar to those accelerated by an electric field (Horwitz, 1984; Liao et al., 2010).

The energetic ions flowing out of the auroral oval into the magnetosphere occur mainly during auroral substorms. Kistler et al. (2006) studied statistically the ion composition in the plasma sheet as a function of substorm activity. In particular, they studied whether substorms occurring during magnetic storms are different from substorms in non-storm times. The role of O^+ ions in substorm dynamics is still unresolved. Observations on the one hand have shown that O^+ ions play a significant role in substorm dynamics (Daglis et al., 1990; Korth et al., 2003; Fu et al., 2002; Nosé et al., 2000), while others indicate the O^+ ions have no effects (Lennartsson et al., 1993; Grande et al., 2003; Kistler et al., 2006).

Published by Copernicus Publications on behalf of the European Geosciences Union.

Table 1. Observation intervals.

Date (2001)	UT	XGSE	YGSE	ZGSE	Substorm
13 February	22:00–02:00[a]	3.05 – (−3.73)	−1.99 – (−1.19)	−6.64 – (−0.5)	16:10 UT
23 February	10:00–13:30	3.44 – (−2.92)	−2.52 – (−1.02)	−6.45 – (−1.7)	03:16 UT
16 March	22:00–01:45[a]	−1.1 – (−2.81)	−1.97 – (2.18)	−6.45 – (3.19)	20:55 UT
19 March	04:00–09:00	2.34 – (−2.44)	−3.79 – (−0.99)	−7.04 – (−4.23)	23:28 UT[b]
28 March	20:00–23:30	−2.36 – (−1.76)	−0.83 – (2.75)	−4.6 – (3.96)	nd
23 April	21:30–01:00[a]	0.38 – (−2.87)	−5.38 – (1.08)	−7.41 – (−3.83)	20:54 UT
24 April	04:00–08:00	−0.79 – (4.36)	3.32 – (−0.59)	3.4 – (8.07)	20:54 UT[b]
26 April	09:00–16:00	−2.1 – (0.15)	−0.73 – (0.48)	−6.49 – (7.37)	06:21 UT
1 May	08:00–12:00	1.83 – (4.87)	1.73 – (−1.94)	6.25 – (8.46)	nd
5 June	07:00–12:00	−3.21 – (−3.81)	−15.1 – (10.5)	−5.49 – (−7.28)	03:12 UT
8 June	03:00–09:00	−2.94 – (1.56)	−2.09 – (2.52)	−6.92 – (3.97)	11:07 UT[b]
12 June	22:00–04:00[a]	−2.65 – (2.34)	−0.55 – (1.17)	−6.5 – (5.26)	01:05 UT
14 July	01:00–06:00	3.28 – (0.29)	2.39 – (−4.7)	2.31 – (6.38)	23:43 UT[b]
5 October	04:00–12:00	1.41 – (−2.53)	2.13 – (−1.9)	−6.44 – (7.42)	03:22 UT
7 October	17:00–21:30	3.4 – (−2.07)	−2.71 – (−2.01)	0.98 – (7.14)	13:44 UT
12 October	00:00–08:00	−6.27 – (2.37)	8.84 – (1.01)	−8.01 – (−5.69)	nd
17 October	07:00–11:00	1.02 – (−467)	−3.21 – (−0.05)	4.44 – (8.2)	01:25 UT
19 October	11:15–13:00	2.56 – (3.38)	0.51 – (−1.76)	−6.43 – (−2.95)	08:02 UT
29 October	04:00–06:00	1.14 – (−1.57)	−3.68 – (−2.03)	3.05 – (6.28)	00:30 UT
31 October	04:00–09:00	−1.37 – (1.13)	8.81 – (3.75)	−8.53 – (−7.71)	16:57 UT[b]
2 November	17:00–19:00	1.99 – (2.82)	1.85 – (−1.47)	−6.87 – (−4.33)	13:24 UT
4 November	00:00–08:00	−9.75 – (−7.75)	16.6 – (16.77)	1.08 – (−3.4)	17:52 UT[b]
6 November	22:00–03:00[a]	5.14 – (−2.73)	15.52 – (12.43)	−5.87 – (−7.81)	19:07 UT
9 November	00:00–12:00	−7.01 – (−2.73)	17.7 – (12.6)	−2.2 – (−7.78)	04:26 UT[b]
14 November	00:00–07:00	−3.66 – (−1.31)	16.7 – (13.0)	−5.26 – (−7.73)	20:18 UT[b]
18 November	00:00–08:00	−6.25 – (−5.06)	16.2 – (18.7)	4.66 – (0.28)	16:48 UT[b]
19 November	06:00–12:00	1.69 – (2.42)	6.65 – (−0.49)	−8.22 – (−5.83)	04:57 UT
17 January (2002)	21:00–02:00[a]	−1.03 – (−2.42)	−3.15 – (−3.31)	−4.02 – (−1.88)	15:52 UT
22 February (2002)	21:00–02:00[a]	1.97 – (8.87)	3.29 – (4.40)	7.64 – (8.31)	18:59 UT

[a] day after, [b] day before, nd stands for no WIC data

POLAR Tide experiment together with Ultraviolet Imager auroral images have established that the outflowing O^+ ions are dependent on the substorm intensity, with outflowing fluxes increasing as the substorm intensity increases (Wilson et al., 2004). We have examined if the substorms are the only source of auroral ions flowing out of the auroral oval. In this article, we show evidence that auroral ions do not only escape during substorms but also during periods without substorms. Periods without substorms include "quiet" arcs, TPAs and pseudo-breakup auroras. This article will focus only on observations during quiet arcs and pseudo-breakup auroras.

A pseudo-breakup aurora is different from a regular substorm breakup. Pseudo-breakup auroras involve activation of a small area of an arc that does not expand globally (Elvey, 1957). In pseudo-breakup auroras, a section of an arc brightens "momentarily" and then fades. This process can occur many times, but this behavior is different from a regular substorm breakup, which includes the growth, expansion and recovery phases (Akasofu, 1964; McPherron, 1970). While a distinction is made between substorms and pseudo-breakups, numerous studies from ground and space have shown that pseudo-breakup auroras include all of the same features associated with auroral substorms, except the intensities are weaker. For example, Pi2 magnetic oscillations, which signify the onset of a substorm, are observed with the brightening of pseudo-breakup auroras but the amplitudes are smaller (Koskinen et al., 1993). In the geomagnetic tail, the magnetic field undergoes "limited" dipolarization, accelerating electrons to several hundred kiloelectron volts and ions to a few megaelectron volts but the fluxes are lower (Fillingim et al., 2001; Parks et al., 2001). This article will add another feature to the list of pseudo-breakup auroras: acceleration of H^+, O^+ and He^+ ions upward out of the auroral oval ionosphere, in a nearly identical way to ions accelerated along the magnetic field in regular substorms.

The outflowing ions during periods without substorms have been measured by the ion composition experiment known as Composition Distribution Function (CODIF) on Cluster (Rème et al., 2001). Periods of substorms and those without substorms are determined using auroral images obtained by the Wideband Imaging Camera (WIC) on the IMAGE spacecraft (Mende et al., 2000) aided by the list of substorm onsets identified by Frey et al. (2004), Auroral Electrojet (AE) indices (from the World Data Center for Geomagnetism, Kyoto AE index service) and ground-based all-sky camera records of the aurora obtained by MIRACLE (Magnetometers – Ionospheric Radars – All-sky Cameras Large Experiment) in northern Scandinavia.

A random survey of ion composition data from Cluster (Rème et al., 2001) for 30 different days (Table 1) has revealed that most of the outflowing ions occurring during periods without substorms are associated with the auroral oval whose activities included the quiet arcs and pseudo-breakup auroras. The measured energies of the escaping O^+ ions are typically $\sim$ 20–40 eV, but after correcting for the spacecraft potential, the ion beams have energies of $\sim$ 40 to 80 eV. These potentials are lower than the typical potentials associated with substorms which are > 100 eV to several kiloelectron volts (Wilson et al., 2004; Marklund et al., 2010; Cui et al., 2010).

Cluster measured the ions flowing out at heights of $\sim 2\,R_E$ to $> 10\,R_E$. The fluxes of outflowing ions are estimated to be $> 10^3$–$10^5\,\mathrm{cm^{-2}\,s}$. Assuming the source of these ions is the auroral oval area sampled by the WIC, the estimated flow rate of ions during periods without substorms is $\sim 10^{20}\,\mathrm{s^{-1}}$. Noting however that quiet arcs and pseudo-breakup auroras can persist for hours, our results show that the non-substorm contribution of the ions we measure can be very significant for the plasma sheet. We have mapped the footprint of Cluster 3 using Tsyganenko 89 and 96 models to show that the spacecraft are located in the auroral oval. By comparing our results with those in Nilsson et al. (2010) and with the discussion in Nilsson et al. (2013), one may find that not much heating and centrifugal acceleration is expected along these outflow paths in the near-Earth lobes to the plasma sheet. The auroral ions have similar and different features from the ions in the polar wind, upwelling ions (cleft ion fountain) and polar cap (Yan and André, 1997; Maggiolo et al., 2006, 2011; Nilsson et al., 2006). In this first report, we will show three examples from periods with different geomagnetic disturbance levels under which the ion beams were observed flowing out of the ionosphere. Ions from both day and night sides flow out but we do not distinguish between them here, nor will the observations be compared to acceleration models (Yan and André, 1997; Nilsson et al., 2008).

2 Observations

The list of events shown in Table 1 includes the time intervals of the events, the position of Cluster covered during the interval (first number in X, Y, Z represents start position and the number that follows in parenthesis is the end position), and the time of the last substorm that occurred just before the observations started, based on available WIC images (Frey et al., 2004) and AE data. As can be seen, the observation intervals did not include any substorm activity and they generally

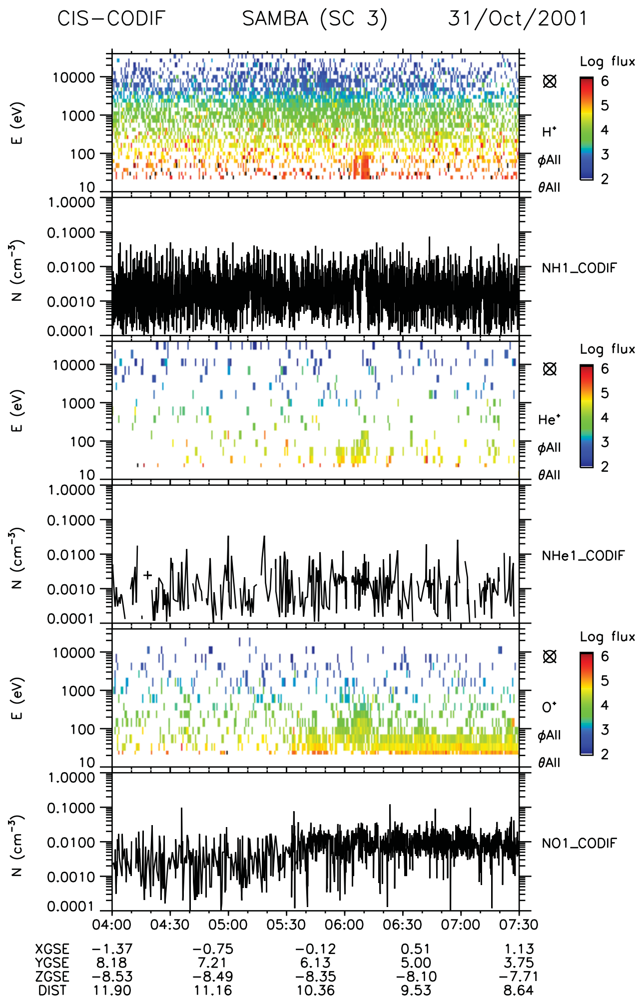

Figure 1a.

started at least several hours after a substorm had occurred. Three examples from this list are presented for further discussion: 31 October 2001, 19 March 2001 and 19 November 2001 (Fig. 1).

In Fig. 1a, b and c, panels 1, 3 and 5 show the differential number flux spectrograms of H^+, He^+ and O^+ ions with energies of $\sim$ 25 eV–40 keV per charge, panels 2, 4 and 6, the density of these ions (statistically significant number counts measured by the instrument corresponds to densities $\geq 0.01\,\mathrm{cm^{-3}}$). The overlapping IMF components and AE indices for these times are shown in Fig. 2a, b and c. The IMF B_z component on 31 October was predominantly negative but small; on 19 March 2001 it was also negative from 04:00 to 06:00 UT after which it became positive (data missing from 07:30 to 09:00 UT); and on 19 November 2001 it fluctuated between positive and negative values. The IMF behavior here indicates that the events we discuss are different from periods when the polar cap beams flow out (Maggiolo et al., 2006; Nilsson et al., 2006).

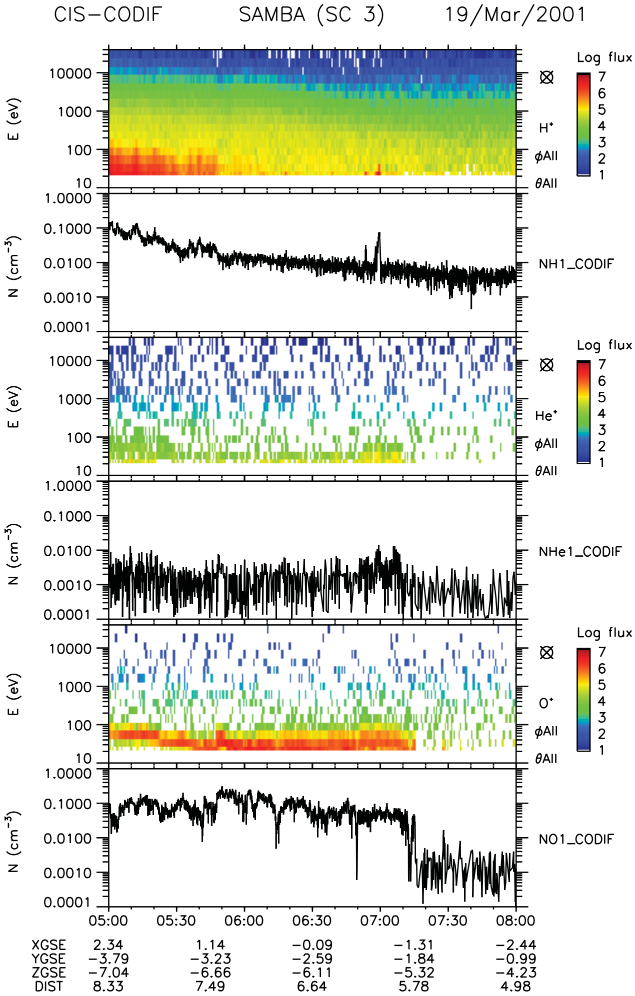

Figure 1b.

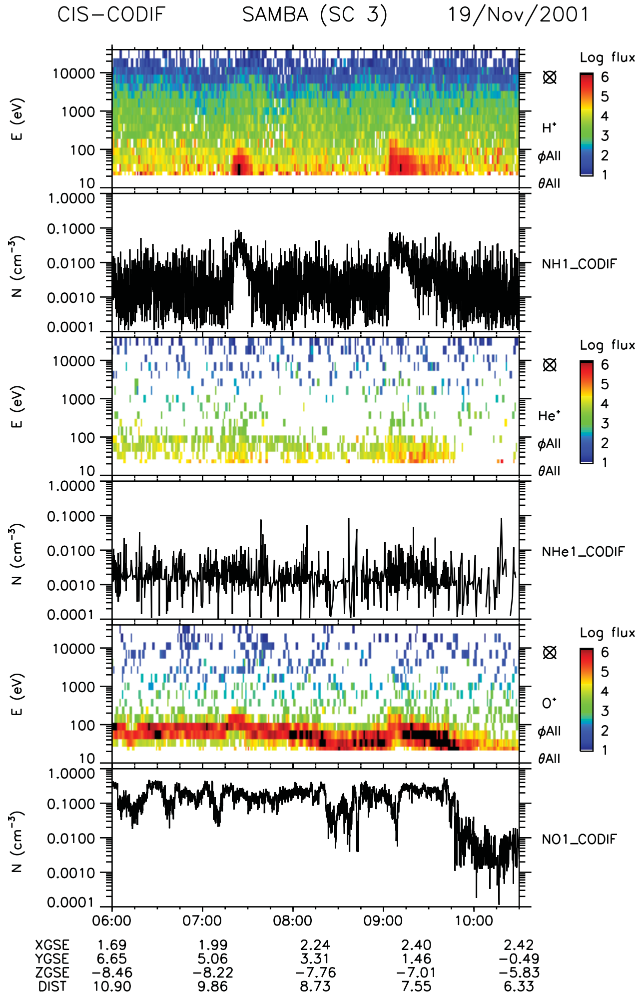

Figure 1c. Three examples of low-energy ions flowing out of the ionosphere during periods without substorms for different levels of geomagnetic disturbances that included quiet arcs and pseudo-breakup auroras. Panels 1, 3 and 5 show the differential number flux spectrograms of H^+, He^+ and O^+ and panels 2, 4 and 6 show densities of these ions. The data shown come from SC3 but the ions were also observed by SC1 and 4.

The keograms covering the same period constructed from the individual WIC Far Ultraviolet Imager images are shown in Fig. 3a, b and c. In each keogram, the top panel shows the auroral intensity as a function of MLat, the second panel as a function of magnetic local time (MLT), and the third panel the integrated photon flux averaged over 18:00–06:00 MLT and 50–80° MLat. The solid black lines are footprints of Cluster 3 in the Southern Hemisphere using T89 and T96 models (the two models essentially gave the same results) for 31 October, 19 March and 19 November 2001 (caveat: the keograms come from auroras in the Northern Hemisphere). The footprints of Cluster on 31 October were at MLat > 80° so are not shown. Figure 4a, b and c shows examples of individual auroral images to illustrate the activities in the auroral oval and pseudo-breakup auroras. Examples of the velocity space distribution of O^+ ions for the three days are shown in Fig. 5. Figure 6 shows the velocity distributions of the three ion species (H^+, He^+ and O^+), all from 19 November 2001.

31 October 2001: On this day, no significant H^+ and He^+ were measured. Only O^+ ions were measured with very low density $\sim 0.01\,\mathrm{cm}^{-3}$ after ∼ 05:40 UT. The keogram (Fig. 3a) shows no significant auroral fluxes until about 06:30 UT. The average fluxes corresponded to ∼ 350 rayleighs (R) at 04:00 UT which increased to 500 R at 06:30 UT. The AE indices between 04:00 and 06:30 UT were nearly zero (Fig. 2a), corroborating the keogram plot. The WIC has a spatial resolution of ∼ 50–70 km, hence auroral arcs are not spatially resolved. Thus, the WIC observations have been augmented using all-sky camera records from MIRACLE. For this day, we find quiet auroral arcs, measured at 557.7 nm, present until ∼ 03:00 UT when the observations ended. There were no substorms recorded (not shown).

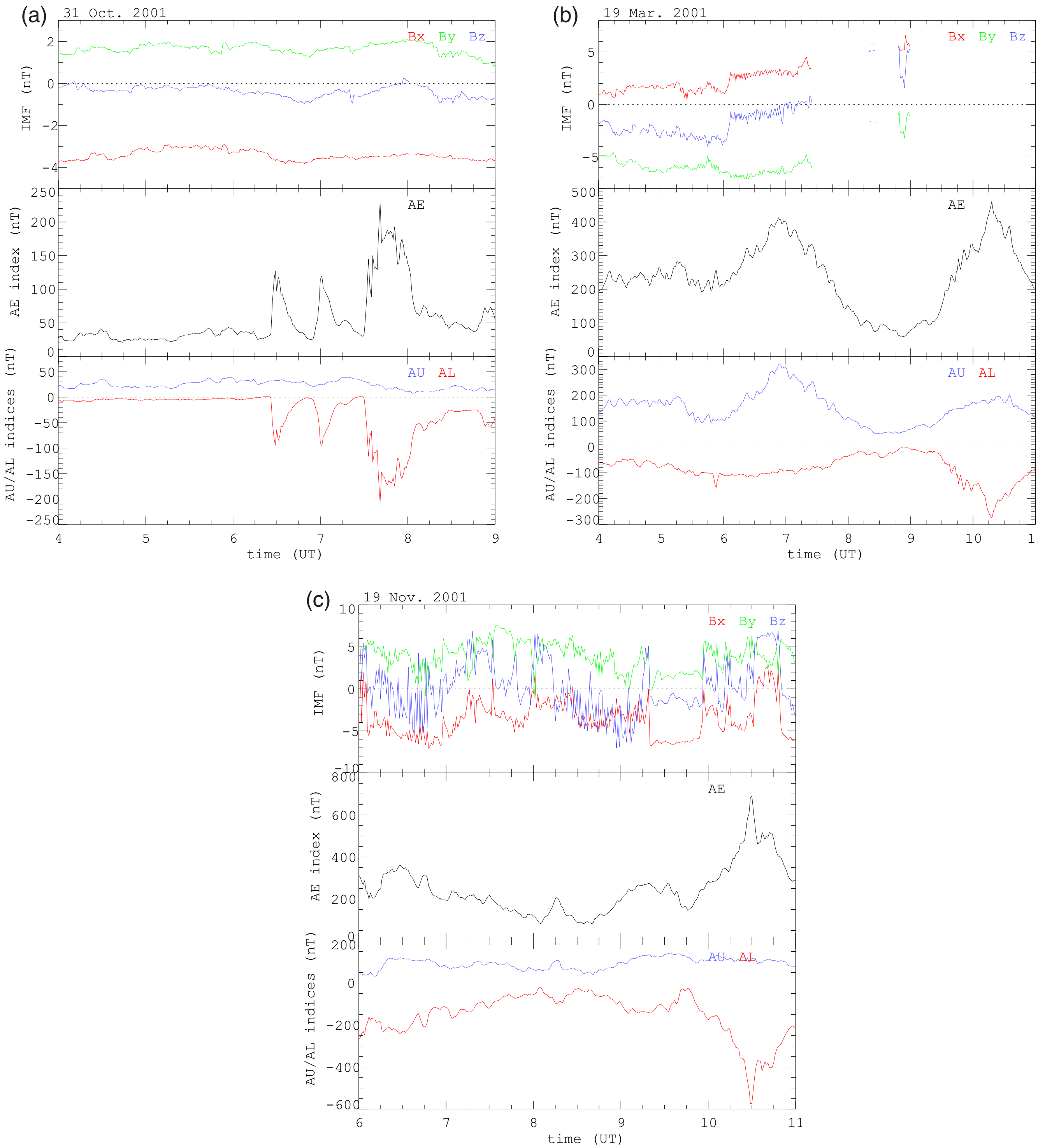

Figure 2. Interplanetary magnetic field (IMF) B_x, B_y and B_z, and AL, AU and AE indices covering the time period of low-energy ion observations shown in Fig. 1.

Individual auroral images (Fig. 4a) show that the small auroral intensity increases observed at 06:30 UT and 07:00 UT occurred near midnight meridian at ∼ 70° MLat and were due to brightening of the aurora and pseudo-breakups, which increased the AL indices to a peak value of ∼ 50 nT. The increased auroral fluxes at ∼ 07:40 UT are due to a more intense pseudo-breakup aurora which increased the AL index to ∼ 100 nT (Fig. 3a). However, no expansion occurred

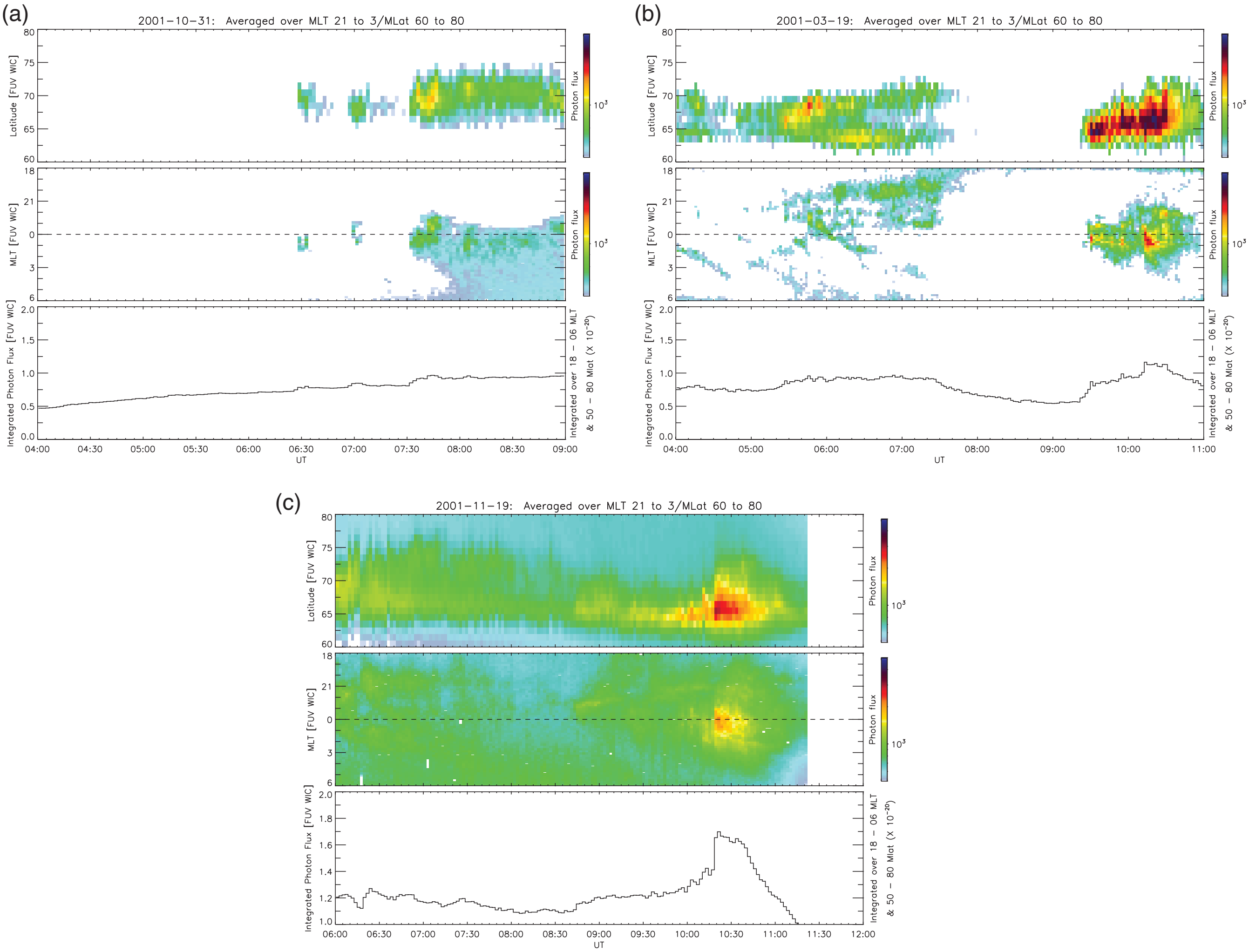

Figure 3. Keogram for 31 October 2001, 19 March 2001 and 19 November 2001 constructed from individual WIC images obtained by IMAGE. The top panel shows the precipitated fluxes as a function of the magnetic latitude (MLat), the middle panel as a function of the magnetic local time (MLT) and the bottom shows integrated photon fluxes from 18 to 06 MLT. During periods without substorms, only quiet arcs and pseudo-breakup auroras are observed.

and hence this intensification was considered due to pseudo-breakup activity.

19 March 2001: Unlike 31 October 2001, significant fluxes were measured in all of the ion species, H^+, He^+ and O^+, between 05:00 and 07:00 UT (Fig. 1b). The density of H^+ started out at $\sim 0.1\,cm^{-3}$ at 05:00 UT which decreased to $0.01\,cm^{-3}$ at 06:30 UT. The He^+ fluxes were weak with densities of $< 0.01\,cm^{-3}$, which however occasionally reached $\sim 0.01\,cm^{-3}$. The O^+ fluxes were the highest with the density around $0.1\,cm^{-3}$ from 05:00 to 07:15 UT.

The geomagnetic activity was also slightly higher than the previous example. The keogram for this day (Fig. 3b) indicates that auroral activity between 04:00 and 08:00 occurred from 62.5 to 70° MLat (top panel) and the activity was in the evening and morning sectors (middle panel). The integrated photon fluxes (bottom panel) corresponded to $\sim$ 550–1000 R between 04:00 and 09:00 UT. Note that Cluster footprints initially traversed the region with small auroral fluxes ($\sim$ 07:00–09:30 UT). Cluster then traversed regions with slightly enhanced intensity, observed around 09:40 UT, resulting in a 200 nT AU increase (Fig. 2b). These auroral fluxes are associated with pseudo-breakup aurora, which included isolated activities at the northern and southern boundaries of the auroral oval, but no substorm expansion occurred (Fig. 4b). According to Frey et al. (2004), a substorm on 19 March 2001 occurred at 09:25 UT and the prior substorm was on 18 March 2001 at 21:27 UT (not shown). A substorm growth phase was observed beginning around 09:15 UT (see the keogram) that led to substorm onset at 09:25 UT (Fig. 2b, 3b, 4b).

19 November 2001: Figure 1c shows the differential number flux spectrograms of the species H^+, He^+ and O^+

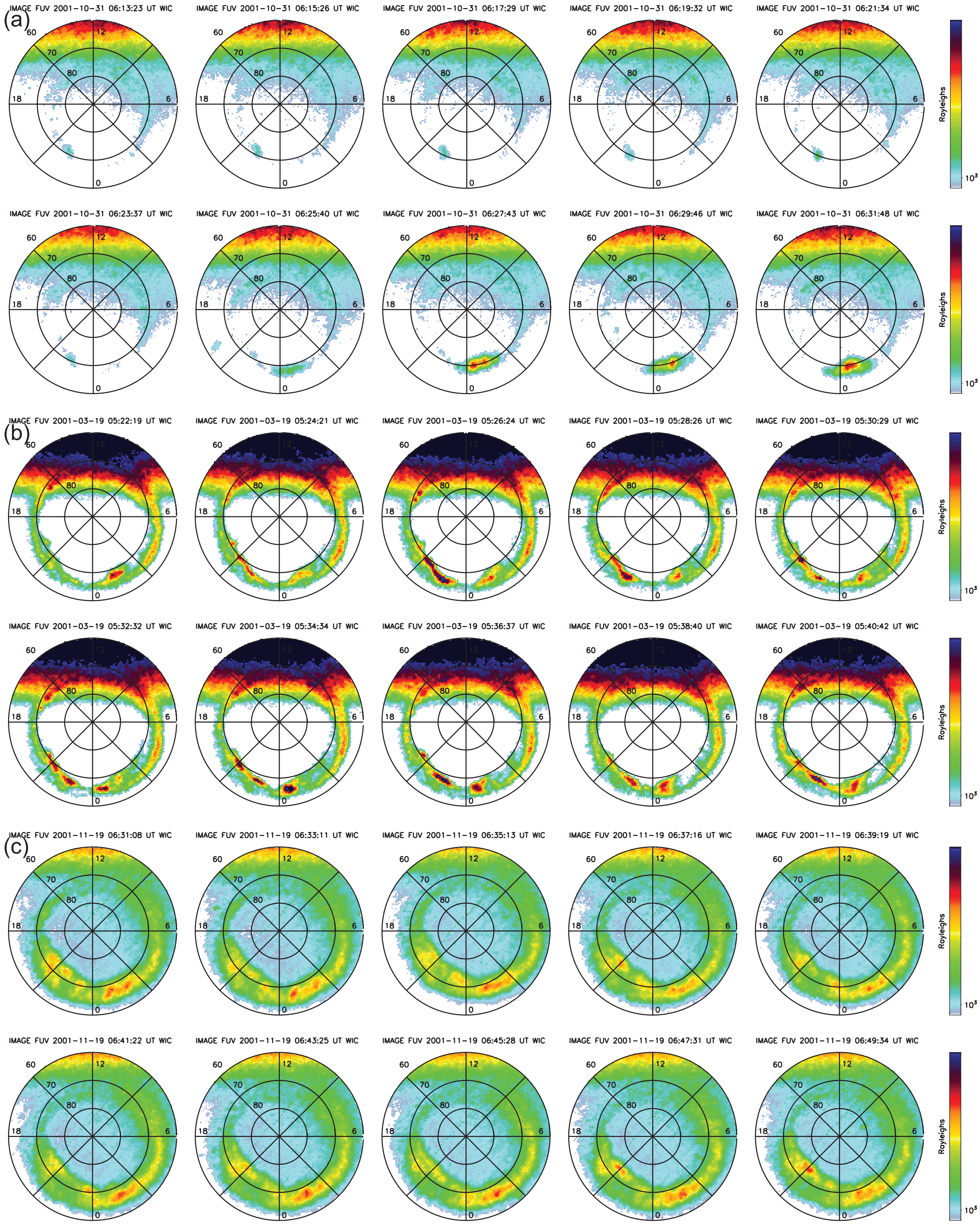

Figure 4. Individual auroral images for illustrating the type of activity observed for the three days, 31 October (**a**), 19 March (**b**) and 19 November 2001 (**c**) that cover the period of low-energy ion observations. The intensity of the aurora is shown in rayleighs.

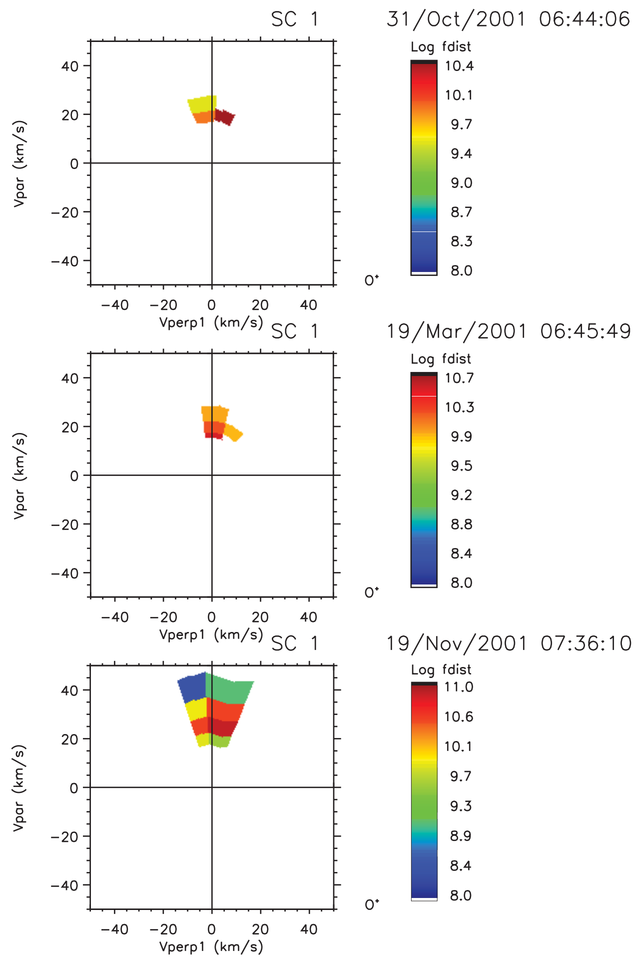

Figure 5. An example of velocity space distributions of O^+ ions measured on 31 October 2001, 19 March 2001 and 19 November 2001. These distributions are shown according to the spacecraft's coordinate system and the velocity space is defined in terms of velocities parallel (V_{par}) and perpendicular (V_{perp}) to the magnetic field direction. The scales are $\pm 50\,km\,s^{-1}$. The beams were also observed by SC3 and 4.

(06:00–10:00 UT). The H^+ density was $\sim 0.08\,cm^{-3}$, O^+ density $0.32\,cm^{-3}$ and He^+ density $< 0.01\,cm^{-3}$. This and the last example show that the O^+ ions dominated H^+ ions, though not all cases show this tendency. We calculated and averaged the ratios O^+/H^+ for each of the 24 events we examined that had simultaneous WIC images and Cluster ion data. This resulted in half of them having an average ratio O^+/H^+ of $\sim 2.46 \pm 1.57$ and the other half having a ratio of $\sim 0.08 \pm 0.04$ (not shown). The ratios of O^+/He^+ were all > 1 with the average equaling ~ 25, except for two cases. Our observations are different from previous observations (for example FAST) where H^+ ions generally dominated (Möbius et al., 1998; Maggiolo et al., 2006). However, FAST observations came from disturbed substorm times, and the Maggiolo et al. results are from statistical studies. Note that in rare cases, He^+ ions dominate H^+ and O^+ ions (Lund et al., 1998).

Of the three examples, this day (19 November 2001) was the most disturbed with the average integrated photon fluxes starting out around 1.25 kR until $\sim$ 10:30 UT, when a substorm onset occurred (also identified by Frey et al. (2004)). The keogram shows (Fig. 3c) moderate auroral activity during 06:00–10:00 UT with pseudo-breakup activities indicated by the individual images (Fig. 4c; comparison of the first and fourth images shows a spot at 21 MLT disappearing and reappearing again). The AE for $\sim$ 10:30 UT substorm peaked around 500 nT (Fig. 2c), and the individual auroral images show an expansion of the aurora (not shown). For this day, the footprints of Cluster were mapped to the latter part of the auroral activity, hence we have no direct information on the regions of the pseudo-breakup activity.

Distribution function: Figure 5 shows examples of the velocity space distributions of O^+ observed for the three days discussed above. Ion beams are observed by all three Cluster spacecraft (SC1, 3, and 4) but we only show data from Cluster 1. These are 2-D cuts of the 3-D distributions presented in the spacecraft frame where the coordinates are relative to directions parallel (V_{par}) and perpendicular (V_{perp}) to the magnetic field. The scales of the x and y axes are $\pm 50\,km\,s^{-1}$. On these three days, Cluster was traversing the Southern Hemisphere, and the positive V_{par} corresponds to ions flowing parallel to the magnetic field direction out of the ionosphere. All of the ions are field-aligned beams occupying a very small region of the velocity space (one or two pitch-angle bins closest to the direction of $\boldsymbol{B}$), and the measured O^+ beams have a velocity of $\sim 20\,km\,s^{-1}$ (for spacecraft potential correction, see below).

While the O^+ beams can form from velocity filter effects (Liao et al., 2010, 2012; Nilsson et al., 2004), we will interpret our observations in terms of particle acceleration by parallel potential drops because the distributions we measured were very much confined to the parallel direction (Marklund et al., 2010). In this case, the energy per charge of an ion that has gone through a potential drop $\Delta\phi$ measured by CODIF is $mv^2/2q = (W_{th}/q) + \Delta\phi$, where W_{th} is the thermal energy. If the initial thermal energy of the ambient ionospheric plasma (< 1 eV) is assumed to be much less than the potential drop ($W_{th} \ll q\,\Delta\phi$), then the shift of the peak of the ion beam will correspond to the energy gained by going through the potential drop. The observed beam velocities of $20\,km\,s^{-1}$ indicate the O^+ ions have undergone a potential drop of $\sim$ 20–40 V $\Delta\phi = mv^2/2q = 16 \times 1.6 \times 10^{-27} \times (20 \times 10^3)^2/2 \times 1.6 \times 10^{-19} = 32$ V along the magnetic field. However, the spacecraft was charged positively to $\sim$ 10–40 V, indicating the actual beam energy is $\sim$ 50–80 V.

Figure 6 shows the velocity space distributions of the ions measured on 19 November 2001. The measured velocity of the H^+ beam is $\sim 100\,km\,s^{-1}$, of He^+ is $\sim 50\,km\,s^{-1}$ and of $O^+ \sim$ 20–30 $km\,s^{-1}$. The measured ratios of beam velocities V_b of O^+ relative to H^+ is ~ 4 and of $He^+ \sim 2$. These values

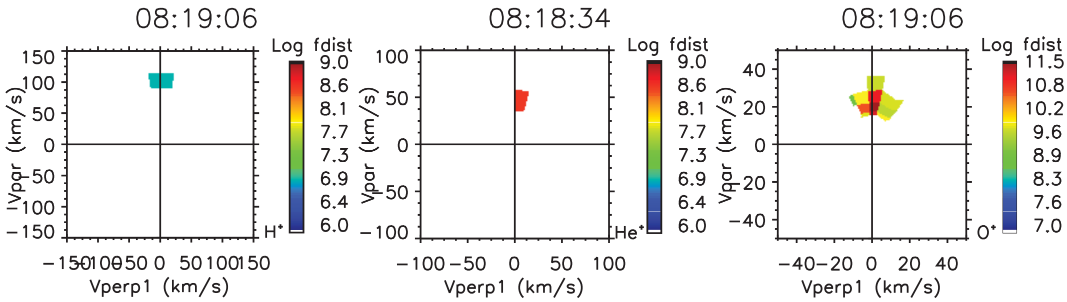

Figure 6. An example of velocity space distributions of O^+ ions measured on 31 October 2001, 19 March 2001 and 19 November 2001. These distributions are shown according to the spacecraft's coordinate system and the velocity space is defined in terms of velocities parallel (V_{par}) and perpendicular (V_{perp}) to the magnetic field direction. The scales are $\pm 50\ km\,s^{-1}$. The beams were also observed by SC3 and 4.

are exactly the same as the theoretical ratios of the beam velocities of O^+ and He^+ relative to the H^+ if all of the ions had gone through the same potential drop: $V_{H^+} = 2V_{He^+}$ and $V_{H^+} = 4V_{O^+}$. Thus, our observations indicate that the three ion species originated from nearly the same height and went through $\sim$ 50–80 V of potential drop. However, note that O^+ ions showed velocities extending to higher values, indicating that O^+ ions went through a larger potential range.

For a Maxwellian distribution, the width of the distribution corresponds to the temperature of the beams, hence our observations show that the temperature of O^+ is larger than H^+ and He^+. The temperature is mass dependent. The estimated temperatures (T) of H^+, He^+ and O^+ ions (in units of kT where k is the Boltzmann constant) using the distribution function are $\sim$ 50, 75 and 200 eV, respectively. The results indicate that ions are not only accelerated by the potential, but they are also heated. Mass-dependent heating has been observed previously (Collin, 1987; Reiff et al., 1988; Möbius et al., 1998; Cui et al., 2010), but the details of how such a heating mechanism works still remains unknown. Note that for the O^+ we observed, there are counts in channels in the adjacent bins relative to the magnetic field direction and the temperature calculation includes their contribution. These particles are probably pitch-angle scattered particles of the original beam along the field. If only the field-aligned portion is included, the temperature will be reduced to < 100 eV. Note also that because of mirror force, the temperature perpendicular to the magnetic field may indicate some heating (see also Nilsson et al., 2012, for Cluster studies of ion heating throughout the polar cap magnetosphere).

3 Discussion

This paper has shown that low-energy ionospheric O^+ ions flow out during periods without substorms. The O^+ ions are originating from the auroral oval populated by quiet arcs and pseudo-breakup auroras. The ion beams are observed by all Cluster spacecraft although the details are different, indicating the structures are smaller than the SC separations (a few hundred kilometers). Preliminary results of test particle simulation using Tsyganenko model (Tsyganenko and Sitnov, 2007) with a Weimer electric field (Weimer, 2001) show these ions end up in the lobe and plasma sheet (not shown). However, the results depend on the convective field, which is not measured, and require further studies. Our observations are consistent with previous results that indicate that O^+ ions are expected to end up in the plasma sheet (Haaland et al., 2012).

A qualitative picture that is emerging from these preliminary observations is that the field-aligned O^+ ions are accelerated along the magnetic field direction by a potential drop very similar to ions accelerated during substorms (Marklund et al., 2010). The observed values of the streaming velocity ratios of H^+/O^+ and H^+/He^+ support the field-aligned acceleration interpretation. However, as noted earlier, a competing mechanism for producing field-aligned beams is velocity filter effects, which is not excluded (Liao et al., 2010; Nilsson et al., 2004). The observed potential for periods without substorms is a few tens of electron volts. The escaping energies and fluxes are a few orders of magnitude smaller than in substorms (Wilson et al., 2004; Yan and André, 1997).

The auroral arcs are not resolved by the WIC, whose spatial resolution is $\sim$ 50–70 km. Thus, it is not known if the source of the low-energy ions includes only the quiet auroral arcs and pseudo-breakup arcs or if it also includes the larger auroral oval. There is freedom about what size we choose for the source area. If we include the area of 18–06 MLT and 50–80 MLat as in the keogram, the size is about $2.8 \times 10^{17}\ cm^2$. If we look at a smaller region near midnight, say 21–03 MLT and 65–75 MLat, the area is only $3.8 \times 10^{16}\ cm^2$, about an order of magnitude smaller. Based on these numbers the escaping fluxes correspond to a flow rate of 10^{19}–10^{21} ions s^{-1}. This number is less than the cold ions escaping the polar cap, 10^{26} ions s^{-1} (Engwall et al., 2009). However, considering that the quiet auroral oval can persist for hours, the number of ions escaping here ($> 10^{24}$ ions) can be higher than that predicted by Seki et al. (2001) and comparable to the number of energetic ions escaping during substorms (Yan and André, 1997).

This article has focused only on the auroral oval that included quiet arcs and pseudo-breakup auroras. However, auroras during periods without substorms also include TPAs, observed during quiet solar wind conditions when IMF Bz is northward. Superficial comparison of TPAs reported by Kullen (2012) with overlapping FAST ion composition data shows O^+ ions were flowing out in some of the TPA events. The electrons of the TPAs have energy spectra similar to the electrons in the plasma sheet (Meng, 1981), suggesting that TPAs are connected to the plasma sheet. However, what causes plasma sheet electrons to appear in TPAs in the polar cap region is not precisely understood. Observations of TPAs have recently been reviewed in Kullen (2012) and references therein).

A fundamental question that still remains unanswered is why pseudo-breakup auroras do not expand. Substorm onsets require dissipation of energy stored in the geomagnetic tail into the ionosphere, and the ionosphere plays an important role (Lysak, 1990). This has suggested that the reason for the non-expansion is that the coupling between the magnetosphere and ionosphere is not adequate and inhibits current flow. But at this juncture, the details remain unclear. Future investigations of non-substorm auroras together with observations of O^+ ions escaping the ionosphere and radar measurements of ionospheric conductivity (Wahlund et al., 1992; Koskinen et al., 1993) could lead to a better understanding of the coupling of the magnetosphere and ionosphere and the role the ionosphere plays in substorm onset mechanisms.

Acknowledgements. This research work is in part supported by a NASA grant to the University of California Berkeley, NNX11AD49G-2/15. The work by E. Lee was in part supported by the BK21 Plus Program and Basic Science Research Program (NRF-2013R1A1A2010711) through the National Research Foundation funded by the Ministry of Education of Korea.

Topical Editor E. Roussos thanks two anonymous referees for their help in evaluating this paper.

References

Akasofu, S. I.: The development of the auroral substorm, Planet. Space Sci., 12, 273–282, doi:10.1016/0032-0633(64)90151-5, 1964.

André, M. and Yau, A.: Theories and observations of ion energization and outflow in the high latitude magnetosphere, Space Sci. Rev., 80, 27–48, doi:10.1023/A:1004921619885, 1997.

Collin, H. L., Peterson, W. K., and Shelley, E. G.: Solar cycle variation of some mass dependent characteristic of upflowing ion beams of terrestrial ions, J. Geophys. Res., 92, 4757–4762, doi:10.1029/JA092iA05p04757, 1987.

Cui, Y., Fu, S. Y., and Parks, G. K.: Heating of ionospheric ion beams in inverted-V structures, Geophys. Res. Lett., 41, 3752–3758, doi:10.1002/2014GL060524, 2014.

Daglis, I., Sarris, E. T., and Kremser, G.: Indications for ionospheric participation in the substorm processes from AMPTE/CCE observations, Geophys. Res. Lett., 17, 57–60, doi:10.1029/GL017i001p00057, 1990.

Elvey, C. T.: Problems in auroral morphology, Proc. Nat. Acad. Sci. USA, 43, 63–75, 1957.

Engwall, E., Eriksson, A. I., Cully, C. M., André, M., Puhl-Quinn, P. A., Vaith, H., and Torbert, R.: Survey of cold ionospheric outflows in the magnetotail, Ann. Geophys., 27, 3185–3201, doi:10.5194/angeo-27-3185-2009, 2009.

Fillingim, M. O., Parks, G. K., Chen, L. J., McCarthy, M., Spann, J. F., and Lin, R. P.: Comparison of plasma sheet dynamics during pseudobreakups and expansive aurorae, Phys. Plasmas, 8, 1127–1132, doi:10.1063/1.1355679, 2001.

Frey, H. U., Mende, S. B., Angelopoulos, V., and Donovan, E. F.: Substorm onset observations by IMAGE-FUV, J. Geophys. Res., 109, A10304, doi:10.1029/2004JA010607, 2004.

Fu, S. Y., Zong, Q. G., Fritz, T. A., Pu, Z. Y., and Wilken, B.: Composition signatures in ion injections and its dependence on geomagnetic conditions, J. Geophys. Res., 107, 1299, doi:10.1029/2001JA002006, 2002.

Grande, M., Perry, C. H., Hall, A., Fennell, J., Nakamura, R., and Kamide, Y.: What is the effect of substorms on the ring current ion population during a geomagnetic storm?, in: Disturbances in Geospace: The Storm-Substorm Relationship, Geophys. Monogr. Ser., 142, edited by: Sharma, A., Kamide, Y., and Lakahini, G., AGU, Washington, D.C., 75–89, doi:10.1029/142GM08, 2003.

Haaland, S., Eriksson, A., Engwall, E., Lybekk, B., Nilsson, H., Pedersen, A., Svenes, K., André, M., Förster, M., Li, K., Johnsen, C., and Østgaard, N.: Estimating the capture and loss of cold plasma from ionospheric outflow, J. Geophys. Res., 117, A07311, doi:10.1029/2012JA017679, 2012.

Horwitz, J. L.: Features of ion trajectories in the polar magnetosphere, Geophys. Res. Lett., 11, 1111–1114, doi:10.1029/GL011i011p01111, 1984.

Kistler, L. M., Mouikis, C. G., Cao, X., Frey, H., Klecker, B., Dandouras, I., Korth, A., Marcucci, M. F., Lundin, R., McCarthy, M., Friedel, R., and Lucek, E.: Ion composition and pressure changes in storm time and nonstorm substorms in the vicinity of the near-Earth neutral line, J. Geophys. Res., 111, A11222, doi:10.1029/2006JA011939, 2006.

Korth, A., Friedel, R. H. W., Henderson, M. G., Frutos-Alfaro, F., and Mouikis, C. G.: O^+ transport into the ring current: Storm versus substorms, in: Disturbances in Geospace: The Storm-Substorm Relationship, Geophys. Monogr. Ser., 142, edited by: Sharma, A., Kamide, Y., and Lakahini, G., AGU, Washington, D.C., 59–73, doi:10.1029/142GM07, 2003.

Koskinen, H. E. J., Lopez, R. E., Pellinen, R. J., Pulkkinen, T. I., Baker, D. N., and Bösinger, T.: Pseudobreakup and substorm growth phase in the ionosphere and magnetosphere, J. Geophys. Res., 98, 5801–5813, doi:10.1029/92JA02482, 1993.

Kronberg, E. A., Ashour-Abdalla, M., Dandouras, I., Delcourt, D. C., Grigorenko, E. E., Kistler, L. M., Kuzichev, I. V., Liao, J., Maggiolo, R., Malova, H. V., Orlova, K. G., Peroomian, V., Shklyar, D. R., Shprits, Y. Y., Welling, D. T., and Zelenyi, L. M.: Circulation of heavy ions and their dynamical effects in the magnetosphere: Recent observations and models, Space Sci. Rev., 184, 173–235, doi:10.1007/s11214-014-0104-0, 2014.

Kullen, A.: Transpolar Arcs: Summary and Recent Results, in: Auroral Phenomenology and Magnetospheric Processes: Earth and

Other planets, Geophys. Monogr. Ser., 197, edited by: Keiling, A., Donovan, E., Bagenal, F., and Karlsson, T., AGU, Washington, D.C., 69–80, doi:10.1029/2011GM001183, 2012.

Lennartsson, O. W., Klumpar, D. M., Shelley, E. G., and Quinn, J. M.: Experimental investigation of possible geomagnetic feedback from energetic (0.1 to 16 keV) terrestrial O^+ ions in the magnetotail current sheet, J. Geophys. Res., 98, 19443, doi:10.1029/93JA01991, 1993.

Li, K., Haaland, S., Eriksson, A., André, M., Engwall, E., Wei, Y., Kronberg, E. A., Fränz, M., Daly, P. W., Zhao, H., and Ren, Q. Y.: On the ionospheric source region of cold ion outflow, Geophys. Res. Lett., 39, L18102, doi:10.1029/2012GL053297, 2012.

Liao, J., Kistler, L. M., Mouikis, C. G., Klecker, B., Dandouras, I., and Zhang, J.-C.: Statistical study of O^+ transport from the cusp to the lobes with Cluster CODIF data, J. Geophys. Res., 115, A00J15, doi:10.1029/2010JA015613, 2010.

Liao, J., Kistler, L. M., Mouikis, C. G., Klecker, B., and Dandouras, I.: Solar cycle dependence of the cusp O^+ access to the near-Earth magnetotail, J. Geophys. Res., 117, A10220, doi:10.1029/2012JA017819, 2012.

Lund, E. J., Möbius, E., Tang, L., Kistler, L. M., Popecki, M. A., Klumpar, D. M., Peterson, W. K., Shelley, E. G., Klecker, B., Hovestadt, D., Temerin, M., Ergun, R. E., McFadden, J. P., Carlson, C. W., Mozer, F. S., Elphic, R. C., Strangeway, R. J., Cattell, C. A., and Pfaff, R. F.: FAST observations of preferentially accelerated He^+ in association with auroral electromagnetic ion cyclotron waves, Geophys. Res. Lett., 25, 2049–2052, doi:10.1029/98GL00304, 1998.

Lysak, R. L.: Electrodynamic coupling of the magnetosphere and ionosphere, Space Sci. Rev., 52, 33–87, doi:10.1007/BF00704239, 1990.

Maggiolo, R., Sauvaud, J. A., Fontaine, D., Teste, A., Grigorenko, E., Balogh, A., Fazakerley, A., Paschmann, G., Delcourt, D., and Rème, H.: A multi-satellite study of accelerated ionospheric ion beams above the polar cap, Ann. Geophys., 24, 1665–1684, doi:10.5194/angeo-24-1665-2006, 2006.

Maggiolo, R., Echim, M., De Keyser, J., Fontaine, D., Jacquey, C., and Dandouras, I.: Polar cap ion beams during periods of northward IMF: Cluster statistical results, Ann. Geophys., 29, 771–787, doi:10.5194/angeo-29-771-2011, 2011.

Marklund, G., Ivchenko, N., Karlsson, T., Fazakerley, A., Dunlop, M., Lindqvist, P.-A., Buchert, S., Owen, C., Taylor, M., Vaivalds, A., Carter, P., André, M., and Balogh, A.: Temporal evolution of the electric field accelerating electrons away from the auroral ionosphere, Nature, 414, 724–727, doi:10.1038/414724a, 2010.

McPherron, R. L.: Growth phase of magnetospheric substorms, J. Geophys. Res., 75, 5592–5599, doi:10.1029/JA075i028p05592, 1970.

Mende, S., Heetderks, H., Frey, H. U., Stock, J. M., Lampton, M., Geller, S. P., Abiad, R., Siegmund, O. H. W., Habraken, S., Renotte, E., Jamar, C., Rochus, P., Gerard, J.-C., Sigler, R., and Lauche, H.: Far ultraviolet imaging from the IMAGE spacecraft. 3. Spectral imaging of Lyman-α and OI 135.6 nm, Space Sci. Rev., 91, 287–318, doi:10.1023/A:1005292301251, 2000.

Meng, C.-I.: Polar cap arcs and the plasma sheet, Geophys. Res. Lett., 8, 273–276, doi:10.1029/GL008i003p00273, 1981.

Möbius, E., Tang, L., Kistler, L. M., Popecki, M., Lund, E. J., Klumpar, D., Peterson, W., Shelley, E. G., Klecker, B., Hovestadt, D., Carlson, C. W., Ergun, R., McFadden, J. P., Mozer, F., Temerin, M., Cattell, C., Elphic, R., Strangeway, R., and Pfaff, R.: Species dependent energies in upward directed ion beams over auroral arcs as observed with FAST TEAMS, Geophys. Res. Lett., 25, 2029–2032, doi:10.1029/98GL00381, 1998.

Moore, T. E., Chandler, M. O., Chappell, C. R., Comfort, R. H., Craven, P. D., Delcourt, D. C., Elliott, H. A., Giles, B. L., Horwitz, J. L., Pollock, C. J., and Su, Y.-J.: Polar/TIDE Results on Polar Ion Outflows, in: Sun-Earth Plasma Connections, edited by: Burch, J. L., Carovillano, R. L., and Antiochos, S. K., American Geophysical Union, Washington, D.C., 87–101, doi:10.1029/GM109p0087, 1999.

Nilsson, H., Joko, S., Lundin, R., Rème, H., Sauvaud, J.-A., Dandouras, I., Balogh, A., Carr, C., Kistler, L. M., Klecker, B., Carlson, C. W., Bavassano-Cattaneo, M. B., and Korth, A.: The structure of high altitude O^+ energization and outflow: a case study, Ann. Geophys., 22, 2497–2506, doi:10.5194/angeo-22-2497-2004, 2004.

Nilsson, H., Waara, M., Arvelius, S., Marghitu, O., Bouhram, M., Hobara, Y., Yamauchi, M., Lundin, R., Rème, H., Sauvaud, J.-A., Dandouras, I., Balogh, A., Kistler, L. M., Klecker, B., Carlson, C. W., Bavassano-Cattaneo, M. B., and Korth, A.: Characteristics of high altitude oxygen ion energization and outflow as observed by Cluster: a statistical study, Ann. Geophys., 24, 1099–1112, doi:10.5194/angeo-24-1099-2006, 2006.

Nilsson, H., Waara, M., Marghitu, O., Yamauchi, M., Lundin, R., Rème, H., Sauvaud, J.-A., Dandouras, I., Lucek, E., Kistler, L. M., Klecker, B., Carlson, C. W., Bavassano-Cattaneo, M. B., and Korth, A.: An assessment of the role of the centrifugal acceleration mechanism in high altitude polar cap oxygen ion outflow, Ann. Geophys., 26, 145–157, doi:10.5194/angeo-26-145-2008, 2008.

Nilsson, H., Engwall, E., Eriksson, A., Puhl-Quinn, P. A., and Arvelius, S.: Centrifugal acceleration in the magnetotail lobes, Ann. Geophys., 28, 569–576, doi:10.5194/angeo-28-569-2010, 2010.

Nilsson, H., Barghouthi, I. A., Slapak, R., Eriksson, A. I., and André, M.: Hot and cold ion outflow: Spatial distribution of ion heating, J. Geophys. Res., 117, A11201, doi:10.1029/2012JA017974, 2012.

Nilsson, H., Barghouthi, I. A., Slapak, R., Eriksson, A. I., and André, M.: Hot and cold ion outflow: Observations and implications for numerical models, J. Geophys. Res., 118, 105–117, doi:10.1029/2012JA017975, 2013.

Nosé, M., Lui, A. T. Y., Ohtani, S., Mauk, B. H., McEntire, R. W., Williams, D. J., Mukai, T., and Yumoto, K.: Acceleration of oxygen ions of ionospheric origin in the near-Earth magnetotail during substorms, J. Geophys. Res., 105, 7669–7677, doi:10.1029/1999JA000318, 2000.

Parks, G. K., Chen, L. J., Fillingim, M., and McCarthy, M.: Kinetic characterization of plasma sheet dynamics, Space Sci. Rev., 95, 237–255, doi:10.1023/A:1005206701965, 2001.

Reiff, P., Collin, H. L., Craven, J. D., Burch, J. L., Winningham, J. D., Shelley, E. G., Frank, L. A., and Friedman, M. A.: Determination of auroral electrostatic potentials using high- and low-altitude particle distributions, J. Geophys. Res., 93, 7441–7465, doi:10.1029/JA093iA07p07441, 1988.

Rème, H., Aoustin, C., Bosqued, J. M., Dandouras, I., Lavraud, B., Sauvaud, J. A., Barthe, A., Bouyssou, J., Camus, Th., Coeur-Joly, O., Cros, A., Cuvilo, J., Ducay, F., Garbarowitz, Y., Medale, J.

L., Penou, E., Perrier, H., Romefort, D., Rouzaud, J., Vallat, C., Alcaydé, D., Jacquey, C., Mazelle, C., d'Uston, C., Möbius, E., Kistler, L. M., Crocker, K., Granoff, M., Mouikis, C., Popecki, M., Vosbury, M., Klecker, B., Hovestadt, D., Kucharek, H., Kuenneth, E., Paschmann, G., Scholer, M., Sckopke, N., Seidenschwang, E., Carlson, C. W., Curtis, D. W., Ingraham, C., Lin, R. P., McFadden, J. P., Parks, G. K., Phan, T., Formisano, V., Amata, E., Bavassano-Cattaneo, M. B., Baldetti, P., Bruno, R., Chionchio, G., Di Lellis, A., Marcucci, M. F., Pallocchia, G., Korth, A., Daly, P. W., Graeve, B., Rosenbauer, H., Vasyliunas, V., McCarthy, M., Wilber, M., Eliasson, L., Lundin, R., Olsen, S., Shelley, E. G., Fuselier, S., Ghielmetti, A. G., Lennartsson, W., Escoubet, C. P., Balsiger, H., Friedel, R., Cao, J.-B., Kovrazhkin, R. A., Papamastorakis, I., Pellat, R., Scudder, J., and Sonnerup, B.: First multispacecraft ion measurements in and near the Earth's magnetosphere with the identical Cluster ion spectrometry (CIS) experiment, Ann. Geophys., 19, 1303–1354, doi:10.5194/angeo-19-1303-2001, 2001.

Seki, K., Elphic, R. C., Hirahara, M., Terasawa, T., and Mukai, T.: On atmospheric loss of Oxygen ions from Earth through magnetospheric processes, Science, 291, 1939–1941, doi:10.1126/science.1058913, 2001.

Tsyganenko, N. A. and Sitnov, M. I.: Magnetospheric configurations from a high-resolution data-based magnetic field model, J. Geophys. Res., 112, A06225, doi:10.1029/2007JA012260, 2007.

Wahlund, J.-E., Opgenoorth, H. J., Häggström, I., Winser, K. J., and Jones, G. O. L.: EISCAT observations of topside ionospheric ion outflows during auroral activity: Revisited, J. Geophys. Res., 97, 3019–3037, doi:10.1029/91JA02438, 1992.

Weimer, D. R.: An improved model of ionospheric electric potentials including substorm perturbations and application to the Geospace Environment Modeling November 24, 1996, event, J. Geophys. Res., 106, 407–416, doi:10.1029/2000JA000604, 2001.

Wilson, G. R., Ober, D. M., Germany, G. A., and Lund, E. J.: Nightside auroral zone and polar cap ion outflow as a function of substorm size and phase, J. Geophys. Res., 109, A02206, doi:10.1029/2003JA009835, 2004.

Yau, A. and André, M.: Sources of ion outflow in the high latitude ionosphere, Space Sci. Rev., 80, 1–25, doi:10.1023/A:1004947203046, 1997.